ACCELERATING SPECTRAL UNMIXING BY USING CLUSTERED IMAGES

Sebastian Bauer, Eric Winterbauer and Fernando Puente León

Institute of Industrial Information Technology (IIIT), Karlsruhe Institute of Technology (KIT),
76187 Karlsruhe, Germany

ABSTRACT

We propose the usage of a clustering step before the unmixing of hyperspectral images. This circumvents or at least mitigates the drawback of having a large amount of data that has to be processed by taking advantage of the large number of similar pixels and merging similar pixels into clusters. Afterwards, only the cluster centroids have to be unmixed instead of all image pixels. We call this meta-approach *UNmixing of Clustered Image* (UNCLI). It is especially useful for images with large more or less homogeneous regions. Another natural area of application are unmixing algorithms with spectral regularization because the calculation of the abundance map very often is more costly than the calculation of the endmember matrix. The results confirm that clustering the images with appropriate clustering methods and cluster numbers before endmember estimation and unmixing not only requires less calculation time than using the unclustered image, but additionally improves the results of both endmember and abundance estimation in the presence of noise.

***Index Terms*—** Hyperspectral image, unmixing, clustering, regularization, spatial information.

1. INTRODUCTION

The large amount of information present in a hyperspectral image allows for detailed analysis of the considered scene. On the other hand, it requires the use of well-engineered algorithms due to model ambiguities [1], high sensitivity to noise [2] and spectral variability especially in the case of natural substances [3]. The need for such sophisticated algorithms results in an even greater time requirement than simple pixelwise unmixing. This motivates us to search for techniques that can speed up the unmixing of hyperspectral images. Let us consider an image for illustration. Figure 1 shows the structure of the Jasper dataset [4] (data available in [5]), a remotely sensed hyperspectral image. The large river in the middle of the image consists of many similar pixels. Unmixing every pixel would be time-consuming without giving much more information. Instead, it would be reasonable to use only some pixels representing the whole of the river and unmix only these few pixels. The workflow of clustering the image pixels followed by unmixing the clustered pixels will be called UNCLI (*UNmixing of Clustered Image*). In this paper, we propose to use suitably clustered hyperspectral images as input to the unmixing. Each cluster will be represented only by its centroid and not all pixels that belong to it. This results in a greatly reduced image which will be faster to unmix, see Fig. 1. We will analyze the effects of the application of different clustering algorithms and cluster numbers on the unmixing result.

We want to remark that during our work on the idea of unmixing clustered images, we became aware of a short contribution by Parente and Zymnis [6], who followed a related approach, but did not carry out a thorough analysis of the effect of the used clustering algorithm and cluster number on the unmixing results.

2. SPECTRAL UNMIXING

Deterministic unmixing methods are in many cases extensions of nonnegative matrix factorization (NMF). They rely on the minimization of an objective function which in case of the linear mixing models is of the form

$$J(\mathbf{M}, \mathbf{A}) = J_{\text{data}}(\mathbf{M}, \mathbf{A}) + \lambda_1 \mathcal{R}_1(\mathbf{M}) + \lambda_2 \mathcal{R}_2(\mathbf{A}) \quad (1)$$

with the data fidelity term J_{data}. An often used formula is

$$J_{\text{data}} = \|\mathbf{MA} - \mathbf{Y}\|_{\text{F}}^2 \quad (2)$$

using the Frobenius norm $\|\cdot\|_{\text{F}}$. In equation (2), the image matrix $\mathbf{Y} \in \mathbb{R}^{L \times I}$ holds the I measured pixel spectra of length L in its columns. The image is of size $X \times Y$, where $X \cdot Y = I$. The data fidelity ensures that $\mathbf{Y}$ is approximated by the endmember matrix $\mathbf{M} \in \mathbb{R}^{L \times R}$ containing the R endmembers column by column and the abundance matrix $\mathbf{A} \in \mathbb{R}^{R \times I}$ as well as possible. When no regularization is applied ($\lambda_1 = \lambda_2 = 0$), (1) is non-convex and there is no unique solution. For this reason, several regularizers have been proposed to improve the uniqueness of the solution.

Possible choices for the spectral regularizer are, e.g., minimum volume constrained (MVC)-NMF [7], minimum distance constrained (MDC)-NMF [8], minimum endmember-wise distance constrained (MewDC)-NMF [9] and minimium dispersion constrained (MiniDisCo)-NMF [10].

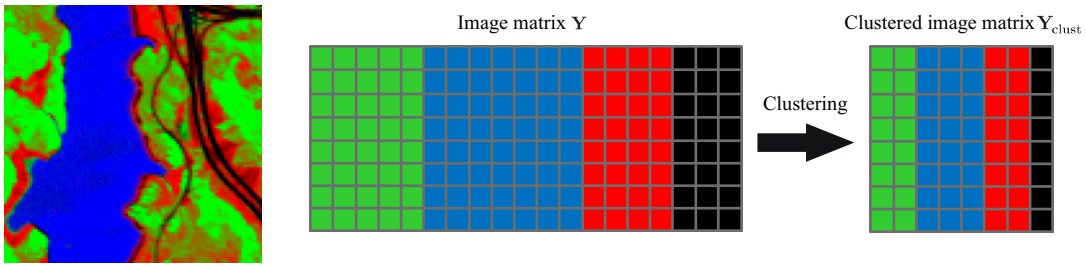

Fig. 1: Ground truth of the Jasper dataset (left; green: tree, red: soil, blue: water, black: road) and corresponding data matrix before and after clustering (middle and right). By clustering, columns of the data matrix belonging to the same category are merged into clusters. As there are less clusters than pixels, the matrix size is decreased.

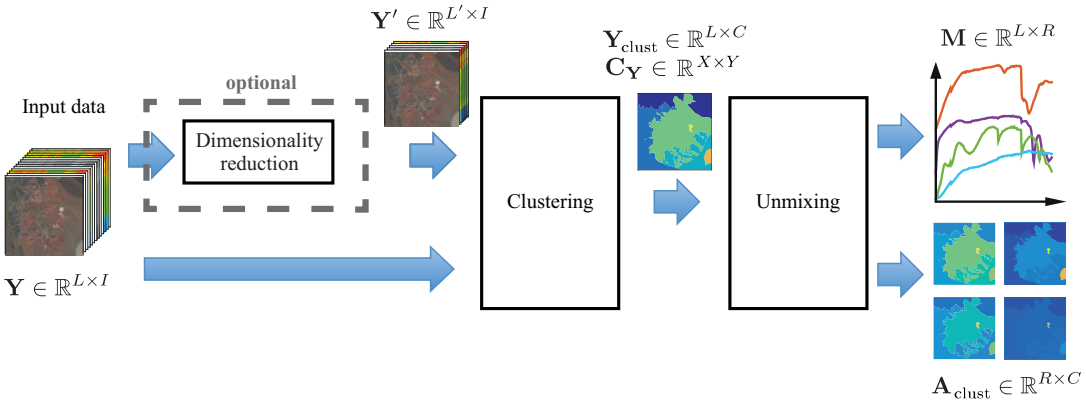

Fig. 2: UNCLI procedure. The goal of the dimensionality reduction is to speed up clustering; for the unmixing step, the non-reduced data are used.

The regularizer $\mathcal{R}_2$ imposing constraints on the abundance matrix has been given more and more attention in the past couple of years, see for example [11, 12].

3. UNCLI PROCEDURE

The detailed workflow of the proposed UNCLI method is shown in Fig. 2. Clustering is performed on the original image data whose spectral dimension can be reduced by an optional dimensionality reduction step consisting of, e.g., principal component analysis (PCA). After clustering, the clustered image is unmixed. The purpose of the spectral dimensionality reduction is the mere acceleration of the clustering; for the unmixing step, the non-reduced data are used.

Figure 2 also shows the used matrices. In case the spectral dimension is to be reduced, the original image $\mathbf{Y} \in \mathbb{R}^{L \times I}$ is reduced to $\mathbf{Y}' \in \mathbb{R}^{L' \times I}$, $L' < L$. The following clustering step provides the segmentation map $\mathbf{C}_{\mathbf{Y}} \in \mathbb{R}^{X \times Y}$ with its elements $\mathbf{C}_{\mathbf{Y},ij} \in \{1, \ldots, C\}$ defining each pixel's mapping to one of the C ($C \in \mathbb{N}$) clusters. From this map, the cluster matrix $\mathbf{Y}_{\text{clust}} \in \mathbb{R}^{L \times C}$ is calculated. It holds the mean spectra of all clusters column by column.

The endmembers present in a scene will be estimated with the endmember extraction algorithms (EEAs) N-FINDR [13] and SISAL [14]. Note that the EEAs are applied to the clustered image. The abundances of the clustered image are calculated pixelwisely with Matlabs `lsqlin` method taking the positivity and abundance sum-to-one constraints into account. In this case, the abundances are calculated only once using the calculated endmembers as initialization. In a separate experiment, we will use the regularizer given by MiniDisCo-NMF representatively for spectral regularization methods.

We tested the following clustering methods: The hierarchical segmentation (HSEG) method [15] allows for both spatial and spectral clustering. The parameter sw (*spclust_wght* in the original source code) balances spatial and spectral clustering; by choosing $sw = 0$, only the spatial neighborhood will be considered, while $sw = 1$ leads to pure spectral clustering. The refined recursive hierarchical segmentation (RHSEG) algorithm [15] overcomes HSEG's drawback of high computational demand in case of spectral clustering. We used the RHSEG implementation given in [16]. ISODATA [17] is based on the k-means algorithm and does not require the number of clusters be defined in advance. The k-means algorithm is also considered. The graph-based image segmentation method developed by Felzenszwalb and Huttenlocher [18] will also be used. We will refer to it as superpixel (SP). For assessing the effect of the aforementioned clustering methods on the unmixing result, it is interesting to include the analysis of the effect of simply averaging the pixels included in small rectangular image areas as a benchmark.

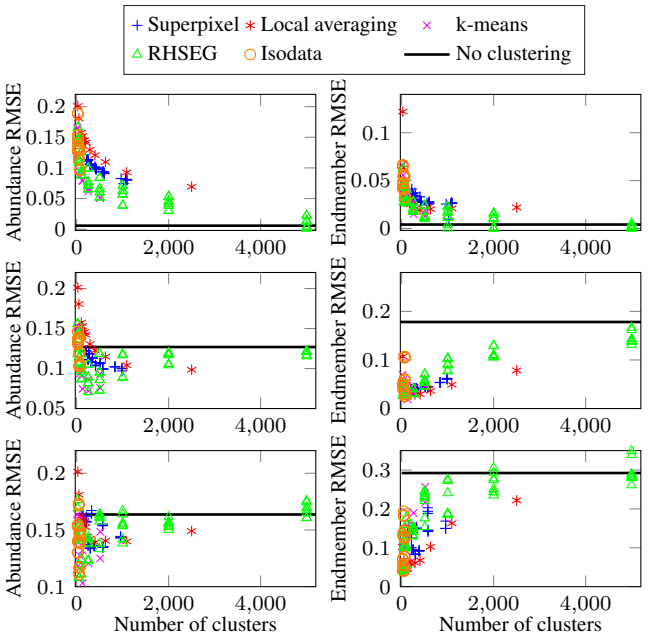

Fig. 3: Unmixing results of Fractal 1 image using SISAL endmember initialization. The solid black line indicates the error that is obtained when the original image without clustering is used. Multiple data points of one algorithm belonging to the same number of clusters represent different parameter combinations. Top row: no noise, second row: 30 dB SNR, third row: 20 dB SNR.

We will refer to this averaging method as local averaging (LA) in the following.

4. RESULTS

For assessing the unmixing results of UNCLI, the first two images of the Fractal dataset [19] will be considered. Two issues will be examined in the evaluation: First, if there is a loss in unmixing accuracy, there should be a gain in processing time. Second, how many clusters should at least be used to have a small error between reconstructed and ground truth abundances?

4.1. Least-Squares Supervised Unmixing

In this section, we will consider supervised unmixing of the clustered Fractal 1 image. For these analyses, the endmembers have been calculated by applying SISAL to the clustered image; the N-FINDR EM initialization (omitted for the sake of space) shows similar results. Figure 3 shows the unmixing results obtained from the clustered image based on the original image with and without noise. It is interesting to note that in the absence of noise, a large number of clusters is required to come close to the results of the unclustered image. However, when the image is degraded by noise, the error is smaller than the one obtained by unmixing the unclustered image. Interestingly, the positive effect of clustering on the endmember spectra is even larger than the one on the abundances.

As we found, the unmixing results of ISODATA and k-means are very similar, so we disregard ISODATA in the following analyses. Due to the shorter calculation time, k-means clustering allows for a larger number of clusters while still being more time-efficient than unmixing all pixels of the original image. The superpixel method interestingly improves the abundance estimation, although the focus is put on spatial clustering which results in cluster centroids consisting of pixels with differing abundances. As long as a minimum number of clusters is considered, UNCLI with RHSEG clustering delivers better results than in the unclustered case. This is independent of the parameter sw defining the ratio of spatial/spectral clustering; however, the more emphasis is put on spectral clustering (sw closer to 1), the better the results. The local averaging method provides the worst results of the abundance estimation, see Fig. 3, but interestingly, the endmember estimation is improved more than with the other clustering algorithms as long as the size of the rectangles within which the mean is calculated is not too large (i.e., there is a sufficient number of clusters and therefore sufficient spatial resolution).

For speeding up the clustering process, it is possible to reduce the spectral dimension of the data by PCA beforehand, see Table 1. It can be seen that the unmixing results obtained using the cluster map derived from the reduced data do not differ greatly from the results using the cluster map resulting from the original data. Note that the reduced data are only used for calculating the cluster map and not for the unmixing process that uses the full spectral dimensionality, see Fig. 2.

Table 1: Minimum unmixing error values with PCA preceding the clustering (abundance and endmember RMSE).

SNR	Clustering	Abu		EM	
		PCA	No PCA	PCA	No PCA
∞	RHSEG	0.003	0.001	1.04×10^{-5}	2.72×10^{-5}
∞	k-means	0.061	0.051	1.31×10^{-2}	1.28×10^{-2}
∞	SP	0.071	0.074	9.19×10^{-3}	9.89×10^{-3}
30 dB	RHSEG	0.068	0.071	2.50×10^{-2}	2.64×10^{-2}
30 dB	k-means	0.070	0.072	3.09×10^{-2}	1.89×10^{-2}
30 dB	SP	0.093	0.097	3.57×10^{-2}	3.72×10^{-2}
20 dB	RHSEG	0.107	0.108	4.08×10^{-2}	3.86×10^{-2}
20 dB	k-means	0.092	0.103	2.85×10^{-2}	3.90×10^{-2}
20 dB	SP	0.132	0.134	7.39×10^{-2}	8.30×10^{-2}

From Fig. 3, it can be seen that clustering the image before unmixing leads to an improvement of the unmixing results. This improvement naturally depends on the number of clusters and on the method; however, the number of clusters can be chosen from a relatively wide range, as it is intuitively clear that too many and too few clusters will not be beneficial.

If clustering and unmixing takes much longer than pure unmixing, there should be at least a gain in accuracy. Ideally, UNCLI results in better results obtained in less time. Figure

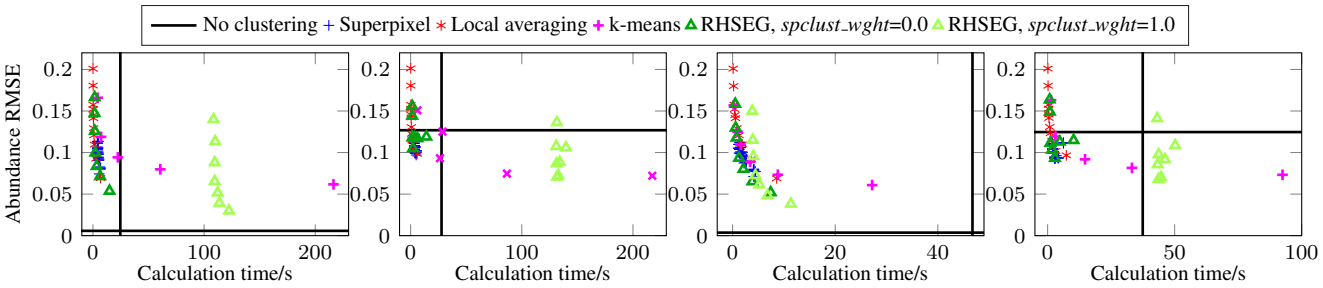

(a) No noise (b) 30 dB SNR (c) PCA, no noise (d) PCA, 30 dB SNR

Fig. 4: Fractal 1: Total calculation time. All four graphs show the abundance RMSE without and with PCA. The solid black lines indicate the error and the time that are obtained when the original image without clustering is used. The desired outcome of UNCLI is that both calculation time and error are below the measures of the unclustered image, i.e., the data points are located in the lower left rectangle of the graph. It can be seen that when UNCLI is used in the case of noise present ((b) and (d)), there is either a gain in accuracy or in calculation time. When RHSEG ($sw = 0$), k-means with a feasible number of clusters or superpixel clustering is used, there is even a gain in terms of both calculation time and accuracy. This shows that UNCLI allows to shift the focus from high time requirement and high accuracy to low time requirement and low accuracy; with the feasible choice of clustering algorithms, even a time decrease and an accuracy increase are obtained simultaneously.

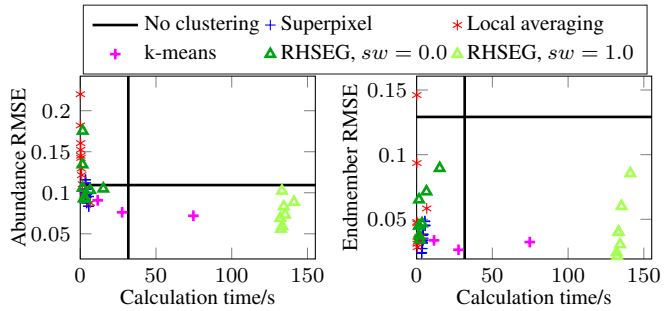

Fig. 5: Fractal 2: Comparison between total calculation time and unmixing quality (SISAL initialization). The solid black lines again represent the unclustered unmixing.

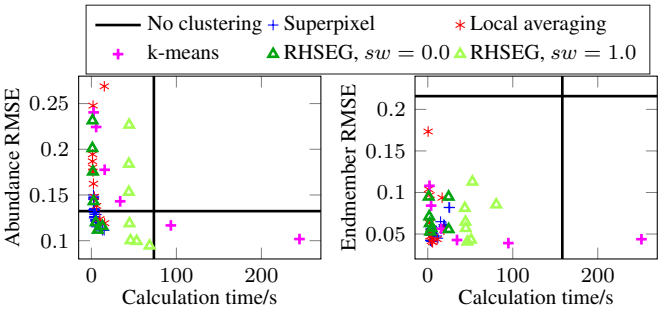

Fig. 6: Fractal 1: Unmixing with MiniDisCo-NMF initialized with SISAL, SNR 30 dB. λ_1 was chosen to 0.5.

4 provides the analysis results.

The results presented in the previous sections are confirmed by Fig. 5 which shows the analysis of the Fractal 2 image. Especially when RHSEG ($sw = 0$), k-means with a feasible number of clusters or superpixel clustering is used, there also is a gain in terms of both calculation time and accuracy.

4.2. Supervised Unmixing with Recalculating the Endmember Spectra Using Spectral Regularization

As stated in the introduction, UNCLI can speed up the unmixing when NMF with spectral regularization is applied. In the following, the MiniDisCo-NMF results will be discussed. Again, the endmembers are initialized by SISAL. PCA was applied before clustering. For comparability, we leave λ_1 constant in our investigations for all cluster numbers. Figure 6 shows the comparison between calculation time and approximation error. Although the benefit is not as large as in Fig. 4, there is the same effect: when the algorithm and the number of clusters are chosen appropriately, there is a gain in both calculation time and abundance estimation. The endmember estimation greatly benefits from clustered images.

5. CONCLUSION

A new unmixing meta-method called UNCLI (UNmixing of Clustered Image) has been proposed. Our analyses show that spectral clustering methods in general perform better than spatial ones; however, all methods can reduce calculation time and increase the unmixing quality when the number of clusters is chosen from a relatively wide range. As it is not possible for us to investigate the combination of all clustering methods with all unmixing methods because of the large amount of possible combinations, the application of UNCLI with the respective unmixing method should be verified first. Future steps could include the weighting of the clusters used during unmixing according to the number of pixels they represent.

6. REFERENCES

[1] Zuyuan Yang, Guoxu Zhou, Shengli Xie, Shuxue Ding, Jun-Mei Yang, and Jun Zhang, "Blind spectral unmixing based on sparse nonnegative matrix factorization," *IEEE Transactions on Image Processing*, vol. 20, no. 4, pp. 1112–1125, 2011.

[2] J.M. Bioucas-Dias, A. Plaza, N. Dobigeon, M. Parente, Qian Du, P. Gader, and J. Chanussot, "Hyperspectral unmixing overview: Geometrical, statistical, and sparse regression-based approaches," *IEEE Journal of Selected Topics in Applied Earth Observations and Remote Sensing*, vol. 5, no. 2, pp. 354–379, 2012.

[3] Ben Somers, Gregory P. Asner, Laurent Tits, and Pol Coppin, "Endmember variability in spectral mixture analysis: A review," *Remote Sensing of Environment*, vol. 115, no. 7, pp. 1603–1616, 2011.

[4] Feiyun Zhu, Ying Wang, Shiming Xiang, Bin Fan, and Chunhong Pan, "Structured sparse method for hyperspectral unmixing," *ISPRS Journal of Photogrammetry and Remote Sensing*, vol. 88, pp. 101–118, 2014.

[5] "Feiyun Zhu, Jasper Dataset," `http://www.escience.cn/people/feiyunZHU/Dataset_GT.html`, Accessed: 2017-02-06.

[6] Mario Parente and Argyris Zymnis, "Statistical clustering and mineral spectral unmixing in AVIRIS hyperspectral image of Cuprite, NV," *CS2009 report, Dec*, 2005.

[7] Lidan Miao and Hairong Qi, "Endmember extraction from highly mixed data using minimum volume constrained nonnegative matrix factorization," *IEEE Transactions on Geoscience and Remote Sensing*, vol. 45, no. 3, pp. 765–777, 2007.

[8] Yue Yu, Shan Guo, and Weidong Sun, "Minimum distance constrained non-negative matrix factorization for the endmember extraction of hyperspectral images," in *International Symposium on Multispectral Image Processing and Pattern Recognition*. International Society for Optics and Photonics, 2007, pp. 679015–679015.

[9] Shaohui Mei and Mingyi He, "Minimum endmember-wise distance constrained nonnegative matrix factorization for spectral mixture analysis of hyperspectral images," in *2011 IEEE International Geoscience and Remote Sensing Symposium (IGARSS)*, pp. 1299–1302.

[10] Alexis Huck, Mireille Guillaume, and Jacques Blanc-Talon, "Minimum dispersion constrained nonnegative matrix factorization to unmix hyperspectral data," *IEEE Transactions on Geoscience and Remote Sensing*, vol. 48, no. 6, pp. 2590–2602, 2010.

[11] M.-D. Iordache, José M. Bioucas-Dias, and Antonio Plaza, "Sparse unmixing of hyperspectral data," *IEEE Transactions on Geoscience and Remote Sensing*, vol. 49, no. 6, pp. 2014–2039, 2011.

[12] José M. Bioucas-Dias and Mário A.T. Figueiredo, "Alternating direction algorithms for constrained sparse regression: Application to hyperspectral unmixing," in *2nd Workshop on Hyperspectral Image and Signal Processing: Evolution in Remote Sensing (WHISPERS), 2010*, pp. 1–4.

[13] Michael E. Winter, "N-FINDR: an algorithm for fast autonomous spectral end-member determination in hyperspectral data," *Proc. SPIE*, vol. 3753, pp. 266–275, 1999.

[14] José M. Bioucas-Dias, "A variable splitting augmented Lagrangian approach to linear spectral unmixing," in *First Workshop on Hyperspectral Image and Signal Processing: Evolution in Remote Sensing (WHISPERS), 2009*, pp. 1–4.

[15] James C. Tilton, "Analysis of hierarchically related image segmentations," in *IEEE Workshop on Advances in Techniques for Analysis of Remotely Sensed Data, 2003*, pp. 60–69.

[16] "NASA's RHSEG Common Software Package," `http://opensource.gsfc.nasa.gov/projects/HSEG/`, Accessed: 2017-02-06.

[17] Geoffrey H. Ball and David J. Hall, "ISODATA, a novel method of data analysis and pattern classification," Tech. Rep., Stanford Research Institute, Menlo Park, CA, 1965.

[18] "Efficient Graph-Based Image Segmentation," `http://sourceforge.net/p/gerbil/svn/65/tree/branches/next/seg_felzenszwalb/`, Accessed: 2017-02-06.

[19] Gabriel Martin and Antonio Plaza, "Region-based spatial preprocessing for endmember extraction and spectral unmixing," *IEEE Transactions on Geoscience and Remote Sensing*, vol. 8, no. 4, pp. 745–749, 2011.